

表面质量控制及检测

## Preparation of Co-doped Silica Sol and Its Application in Sapphire (1120) Polishing

WANG Dan<sup>1a,2</sup>, WANG Wei-lei<sup>2</sup>, QIN Fei<sup>2</sup>, LIU Wei-li<sup>2</sup>, SHI Li-yi<sup>1b</sup>,  
SONG Zhi-tang<sup>2</sup>

(1. a.School of Science, b.Research Center of Nano-science and Nano-technology, Shanghai University, Shanghai 200444, China; 2.Shanghai Institute of Microsystem and Information Technology, Chinese Academy of Sciences, Shanghai 200050, China)

**ABSTRACT:** The work aims to improve polishing rate of A-plane sapphire (1120). Non-spherical and spherical Co-doped silica sol was prepared in induction method and seed induction method, respectively. The two products were applied in chemical mechanical polishing (CMP) of A-plane sapphire. Grain size, morphology, element composition and existential state of product particles were detected with scanning electron microscope (SEM), inductive coupled plasma (ICP) and X-ray photoelectron spectroscopy (XPS). Polishing rate was verified with CP-4 polisher. Surface roughness of polished materials was tested with atomic force microscope. Chemical reaction during polishing process was analyzed based upon XPS test results of polished products. Compared with pure silica sol, non-spherical Co-doped silica sol gave 37% higher polishing rate and similar surface roughness, while spherical Co-doped silica sol had no clear advantage in polishing rate, no evidence showed that Co element was involved in chemical reaction according to XPS results. The positive role of non-spherical Co-doped silica sol in A-plane sapphire polishing is attributed to its shape priority, but not chemical reaction between Al<sub>2</sub>O<sub>3</sub> and Co.

**KEY WORDS:** non-spherical silica sol; cobalt; chemical mechanical polishing; sapphire; COF; XPS

中图分类号: TQ127.2 文献标识码: A 文章编号: 1001-3660(2017)08-0259-09

DOI: 10.16490/j.cnki.issn.1001-3660.2017.08.042

## 钴掺杂硅溶胶的制备及其在 A 向蓝宝石抛光中的应用

王丹<sup>1a,2</sup>, 汪为磊<sup>2</sup>, 秦飞<sup>2</sup>, 刘卫丽<sup>2</sup>, 施利毅<sup>1b</sup>, 宋志棠<sup>2</sup>

(1.上海大学 a.理学院 b.纳米科学与技术研究中心, 上海 200444;

2.中国科学院上海微系统与信息技术研究所, 上海 200050)

**摘要:** 目的 提高 A 向蓝宝石抛光速率。方法 分别采用诱导法和种子法制备了非球形和球形钴掺杂硅溶胶, 并应用于 A 向蓝宝石的化学机械抛光。采用扫描电子显微镜 (SEM)、电感耦合等离子体发射光谱仪 (ICP) 和 X 射线光电子能谱 (XPS) 检测产物颗粒的粒径及其分布、形貌、元素组成及存在状态等, 采用 CP-4 抛光机对抛光速率进行验证, 并用原子力显微镜测试抛光后的材料表面粗糙度, 根据抛光后产物的 XPS 测试结果对抛光过程中的化学反应进行分析。结果 与纯硅溶胶相比, 非球形钴掺杂硅溶胶抛光速率提高了

Received: 2017-03-01; Revised: 2017-04-05

收稿日期: 2017-03-01; 修订日期: 2017-04-05

Fund: Supported by National Natural Science Foundation of China (51205387), Science and Technology Commission of Shanghai (14XD1425300, 14DZ2294900)

基金项目: 国家自然科学基金 (51205387), 上海市优秀技术带头人项目 (14XD1425300, 14DZ2294900)

Biography: WANG Dan (1991—), Female, Master student, Research focus: CMP slurry.

作者简介: 王丹 (1991—), 女, 硕士研究生, 研究方向为纳米抛光液与抛光磨料。

Corresponding author: LIU Wei-li (1975—), Female, Doctor, Researcher, Research focus: CMP slurry.

通讯作者: 刘卫丽 (1975—), 男, 博士, 研究员, 研究方向为纳米抛光液与抛光磨料。

37%，且表面粗糙度相近，而球形钴掺杂硅溶胶抛光速率却无明显优势。XPS 结果显示，目前没有证据表明 Co 元素参与了化学反应。**结论** 非球形钴掺杂硅溶胶在 A 向蓝宝石抛光中起到了积极作用，归因于其形状优势而非  $\text{Al}_2\text{O}_3$  与 Co 之间的化学反应。

**关键词**：非球形硅溶胶；钴；化学机械抛光；蓝宝石；摩擦系数；X 射线光电子能谱

A-plane sapphire, composed of  $\alpha\text{-Al}_2\text{O}_3$ , is widely used in mid-wave infrared-transmitting domes on high-speed missiles and air vehicle windows due to the impressive optical and mechanical properties. All of these applications need high precision surface with low roughness<sup>[1-2]</sup>, so research on the planarization of sapphire attracts much attention. Chemical mechanical polishing (CMP) is a widely accepted method for global planarization, however, lower chemical reaction activity and higher hardness of A-plane sapphire (1120) also post challenges to the CMP material removal rate (MRR).

During CMP process, abrasives have critical effect on the CMP performance due to their shape, hardness, particles size and distribution. Colloidal  $\text{SiO}_2$  has been the mostly used abrasive for the sapphire final CMP process because of the smoother wafer surface<sup>[3]</sup>, but the limited MRR is an urgent problem to be solved. In order to increase MRR of  $\text{SiO}_2$  particles, researches on the optimization of silica abrasives, such as the adjusting particles' size distribution<sup>[4-5]</sup>, unique shape<sup>[6-10]</sup>, modification<sup>[11-12]</sup> and dope<sup>[13-15]</sup> became a hot topic. Among them, preparation of doped silica was first reported by Dong-Wan Kim<sup>[16]</sup>, through the reaction between silicon chloride ( $\text{SiCl}_4$ ) and metal chloride ( $\text{FeCl}_3$ ) in solution. The MRR was found to have increased, the author hold that the slurry system led to the promotion of metal oxide process. In recent years, Co was thought to be efficient for the MRR improvement of C-plane sapphire polishing, and the MRR turns out to be increased with the increasing doping ratio of Co-doped  $\text{SiO}_2$ , according to the research of Ma et al<sup>[17]</sup>.

Metal doped silica is expected to improve the MRR of A-plane sapphire. Thus in this article we choose  $\text{Co}(\text{NO}_3)_2$  as doping agent and induce agent in this article. We fabricated Co-doped colloidal silica by different methods and investigated their CMP performance in A-plane sapphire (1120) polishing. The particles prepared by different methods were found to have different shapes. By comparing the MRR of Co-doped silica and pure silica, we analyzed the effect of cobalt element and the shape of particles. The synthesis methods used in this article are simple, cost effective, and easy for industrializing than that of the previous literature reported.

## 1 Experiments

### 1.1 Materials

Active silicic acid (4.4%, mass fraction, the full text of the same) was prepared by ion exchange method. Cobalt-nitrate hexahydrate ( $\text{Co}(\text{NO}_3)_2 \cdot 6\text{H}_2\text{O}$ ) acted as

the induce agent and doping agent, and sodium hydroxide (0.15%) was catalyst and stabilizer. Deionized water was used in the reaction system. In addition, spherical colloidal silica with 20 nm diameter was provided by Shanghai Xinanna as seeds.

## 1.2 Experiment

### 1.2.1 Preparation of Co-doped colloidal silica by cobalt induced method

The original solution was accomplished by slowly adding 100 mL 2% NaOH solution into 900 mL active silicic acid under stirring. The mixture was heated to 373 K in a four-neck flask, followed by simultaneously dropwise addition of 0.3%  $\text{Co}(\text{NO}_3)_2 \cdot 6\text{H}_2\text{O}$ , 0.15% NaOH and 4.4% active silica acid. It is necessary to keep the pH of the system at 9.0 ~ 11.0 by controlling the drop velocity of NaOH. The obtained Co-doped colloidal silica is named sample A in the text.

Pure colloidal silica was prepared for comparison by the same method except for without cobalt doping, it is named sample B in the text.

### 1.2.2 Preparation of $\text{SiO}_2$ @Co-doped- $\text{SiO}_2$ by seed induced method

$\text{SiO}_2$ @Co-doped- $\text{SiO}_2$  was prepared by seed induced method invented by Pan Ma<sup>[17]</sup>.  $\text{Co}(\text{NO}_3)_2 \cdot 6\text{H}_2\text{O}$ , NaOH, and active silicic acid was added into pure silica seeds simultaneously. The obtained Co-doped colloidal silica is named sample C in the text.

Pure colloidal silica for comparison was prepared by the same method except for without cobalt doping, it is named sample D in the text.

## 1.3 Characterization

The Co-doped colloidal silica obtained was characterized by laser particle size analyzer (Nicomp<sup>TM</sup> 380/ZLS), ICP (inductive coupled plasma, VARIAN 710-ES), metallographic microscope, SEM (focused ion beam, FEI Helios NanoLab 600i), XPS (X-ray photoelectron spectroscopy, ESCALAB 250), and AFM (atomic force microscope, XE-150), among which, Nicomp<sup>TM</sup> 380/ZLS was used to measure the size and zeta potential of the particles via DLS (dynamic light scattering) method; FEI Helios NanoLab 600i with 30~600 000 $\times$  magnification was used to analyzed the morphology of the particles; ICP was applied to detect the content of metal elements (mainly Al and Co) in the system; ESCALAB 250 XPS fitted with a focused monochromatized Al K Alpha was carried out to testify the valence state and the material in the system with the binding energy of C1s (285.02 eV) as reference; metal-

loscope was used to observe defects on wafer surface, and AFM was used to measure roughness of wafer surface.

## 1.4 Polishing test

Polishing tests were conducted by using a CP-4 polishing machine. For all the CMP experiments, 2 inch A-plane sapphires with thickness of 478  $\mu\text{m}$  were used as wafers, and the polyethylene pad was conditioned prior to each polishing test for 5 min. The CMP process parameters are shown in Tab.1.

**Tab.1 CMP process parameters**  
表 1 CMP 过程参数

| Pad   | SUBA-600 |
|---|----------|
| Working pressure/kPa                                    | 41.36    |
| Polishing time/min                                      | 60       |
| Pad rotate speed/( $\text{r}\cdot\text{min}^{-1}$ )     | 100      |
| Wafer rotate speed/( $\text{r}\cdot\text{min}^{-1}$ )   | 90       |
| Slurry supply speed/( $\text{mL}\cdot\text{min}^{-1}$ ) | 125      |

Two groups of abrasives were used in CMP experiments. The first included two kinds of abrasives: Co-doped colloidal silica and pure colloidal silica prepared by cobalt induced method, that is, sample A and sample B. The second included  $\text{SiO}_2@\text{Co-doped-SiO}_2$  and pure silica particles synthesized by seed induced method, which is named as sample C and sample D in the text, respectively. All abrasives were adjusted to a state with pH value of 9.4 and solid content of 10%.

The wafers were cleaned by deionized water and

liquid cleaner, and dried off by air spay gun after being polished. AFM was used to measure the surface roughness of the wafers under tapping mode ( $5\ \mu\text{m}\times 5\ \mu\text{m}$ ). Metallographic microscope was used to observe the defects of the integral wafers.

The material removal rate (MRR) was calculated by weight lose method<sup>[18]</sup>, and the formula is (1).

$$\text{MRR}=(\Delta m\times 10^7)/(\tau\rho\pi R^2) \quad (1)$$

Here the MRR is the material removal rate,  $\text{nm}/\text{min}$ ;  $\Delta m$  is the lose mass of the wafers, g;  $R$  is the radius of the wafers, cm, here  $R=2.54\ \text{cm}$ ;  $\tau$  is the polishing time, min, in the tests,  $\tau=60\ \text{min}$ ,  $\rho$  is the density of the A-plane sapphire,  $3.98\ \text{g}/\text{cm}^3$ .

## 2 Results and discussions

### 2.1 Characterization of the prepared particles

#### 2.1.1 Morphology and size

The morphologies observed by SEM are shown in Fig.1 and the sample A, B, C, D and their corresponding synthesize methods are listed in Tab.2. Compared with sample B, shape of particles in sample A are non-spherical, indicating a possible induce action of  $\text{Co}^{2+}$  during the growth. There are possibly three steps during the formation of non-spherical particles (Fig.1a): nucleation, coalescence and further growth. Firstly, active silicic acid nucleates under a certain temperature. Secondly, with the addition of  $\text{Co}^{2+}$ , counter ion in the absorption layer increases, thus zeta potential, the potential between particle surface and solution, declined,

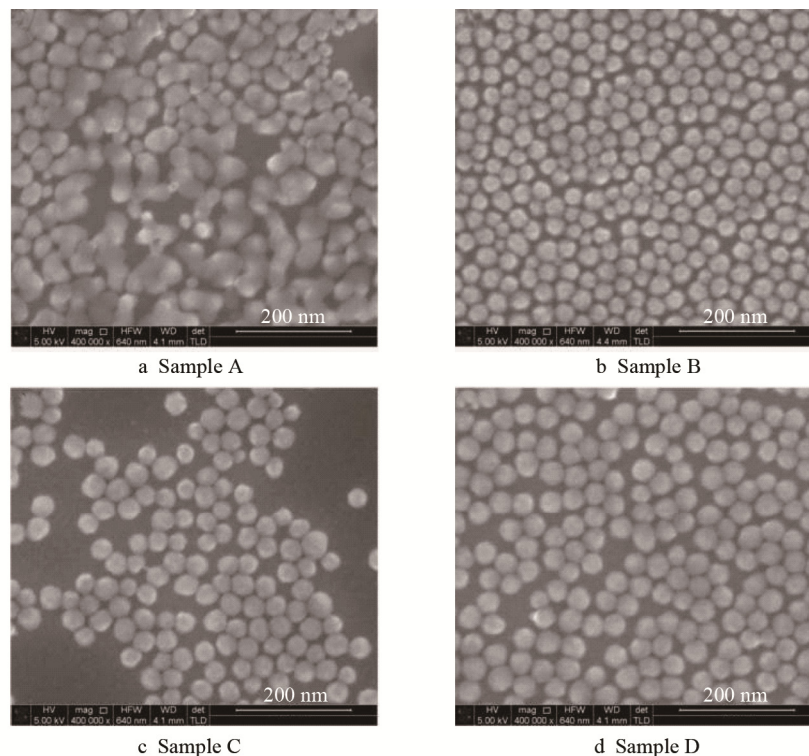


Fig.1 SEM  
图 1 SEM 图

inducing the compression of double electric layer and the coalescence of the nucleus and really small particles. At last, the fused particles become non-spherical during the further growth<sup>[6,10]</sup>.

**Tab.2 Samples and corresponding synthesize methods**  
表 2 样品及其对应的制备方法

| Synthesize method    | Co-doped silica | Pure silica |
|----------------------|-----------------|-------------|
| Co induced method    | Sample A        | Sample B    |
| Seeds induced method | Sample C        | Sample D    |

However, uniform size and shape of particles were found in Fig.1c and Fig.1d, that is SiO<sub>2</sub>@Co-doped-SiO<sub>2</sub> particles (0.37% Co) and pure SiO<sub>2</sub> produced by seed induced method. Particles tend to be more spherical during the following growth period in alkaline solution, especially when the seeds are spherical.

In conclusion, different shapes of Co-doped colloidal silica can be achieved when prepared by different methods described above.

2.1.2 Size of particles

The algorithm applied in DLS method is applicable only when the particles detected are spherical or nearly spherical<sup>[19]</sup>. So here in Fig.2 we present the size and

size distribution calculated from SEM images by nano measure. The average size of Sample C are quite close, which are 37.9 nm and 38.3 nm, respectively. However, the average sizes of sample A and B are different, with that of sample A being 62.41 nm and that of sample B being 32.01 nm, respectively. Such difference is caused by what we said further growth of fused particles.

It's obvious that particles' size distribution of sample A is significantly wider than other samples, with even two peaks. That is caused by the co-existence of fused particles and independent particles during growth. And size distribution of sample B is a little wider than samples synthesized by seeds induced method. The variation value (P. I.) A>B>C>D, partly due to the method and partly due to the existence of Co<sup>2+</sup>.

2.1.3 TEM and Composition

In order to find out where the cobalt exist in the particles, in the water or form independent particles, ICP was applied to the primary liquid of sample A and its supernatant for Co content testing, as is shown in Tab.3.

Undoubtly, Co does exist in silica particles. As is seen from the SEM images, Co doesn't form any independent particles; and cobalt concentration of 0.8104×10<sup>-6</sup> means there was little Co element in the water.

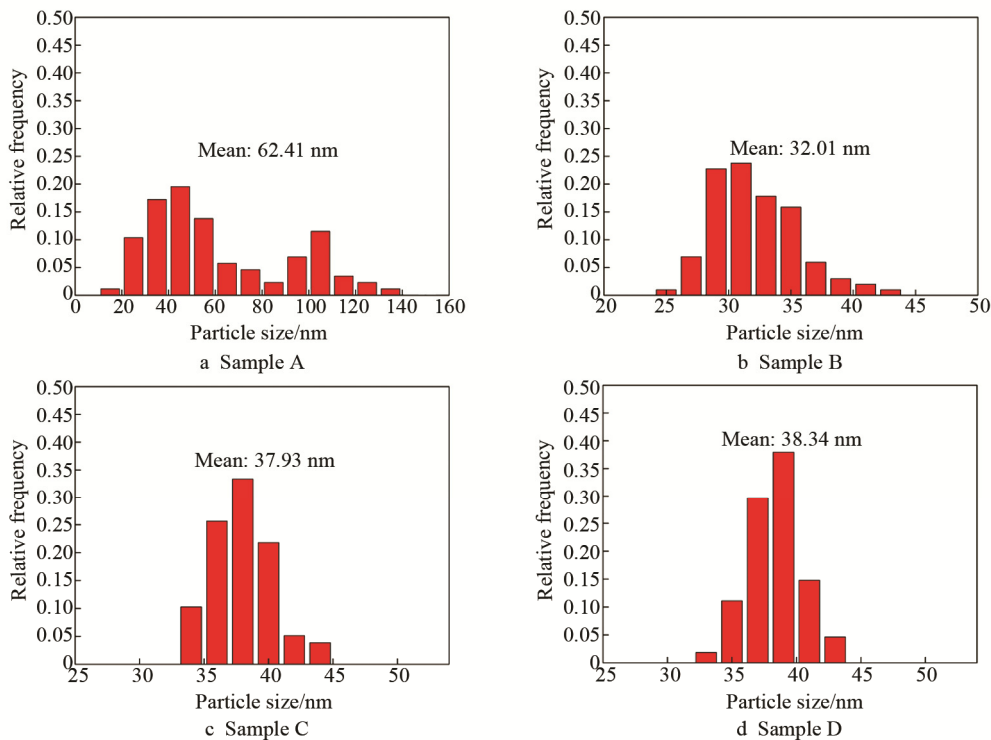


Fig.2 Size and size distribution  
图 2 粒径及其分布

**Tab.3 Cobalt content in sample A and its supernatant liquid**  
表 3 样品 A 及其上清液固含量对比

| Liquid                             | Co-doped silica | Supernatant liquid |
|------------------------------------|-----------------|--------------------|
| Concentration/(×10 <sup>-6</sup> ) | 109.707         | 0.8104             |

Fig.3 shows the TEM image and TEM-EDS spectra of line scan of sample A. Obviously, O and Si show the same change tendency relative to the particle thickness in the scan line, indicating a uniform distribution of O and Si in particles. Since Co content is extremely low, with only 0.5%, the changing tendency of Co is not

as obvious as Si. Having said that, we can see peaks around 75 nm and 50 nm in the magnified spectra still

can be seen. Therefore distribution of Co in particles is confirmed.

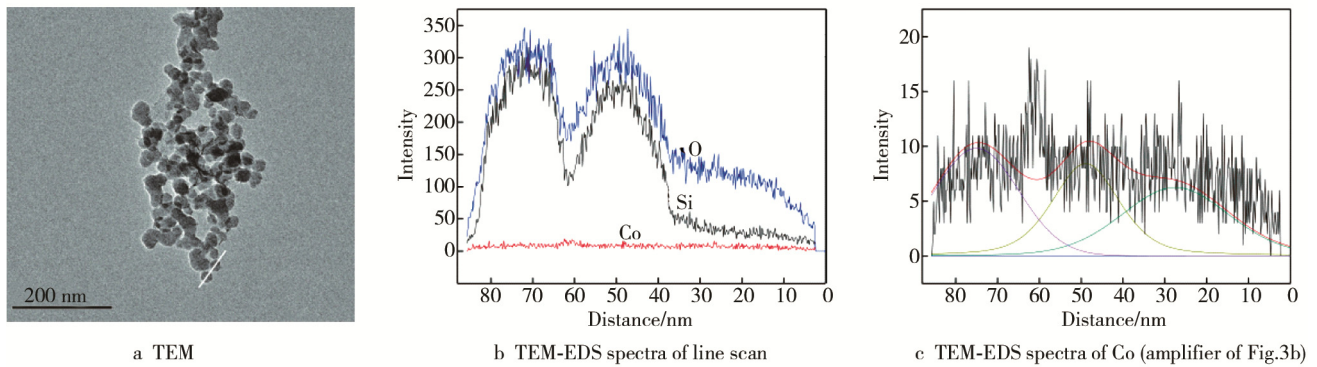


Fig.3 TEM of Sample A  
图 3 样品 A 的 TEM 图

### 2.1.4 Stability

Zeta potential of abrasives is a significant reference for stability of colloids. Generally speaking, the stability of colloid is proportional to the absolute value of zeta potential. It is widely accepted that the colloid is stable enough when the absolute value of zeta potential reaches a certain value, i.e. 30 mV<sup>[20-21]</sup>. And Fig.4 shows the absolute value of zeta potential of sample A and sample B during the growth ( $V_{\text{silicic acid}}$  is the volume of active silicic acid added), the results are between 30 mV and 40 mV, indicating a stable system of Co-doped colloidal silica. And this is proved by the fact that the obtained non-spherical Co-doped silica kept stable in room temperature for 6 months without gelling or precipitating. So it is credible that the non-spherical Co-doped colloidal silica obtained is stable enough for CMP application.

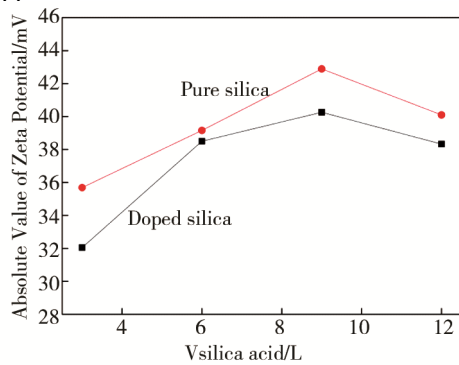


Fig.4 Absolute value of zeta potential of Co-doped colloidal silica (sample A) and pure colloidal silica (sample B) during growth

图 4 生长过程中钴掺杂硅溶胶 (样品 A) 和纯硅溶胶 (样品 B) 的 zeta 电位绝对值

## 2.2 Polishing performance

In terms of Co-doped colloidal silica and pure silica with same size and shape, their MRR in A-plane sapphire polishing has no difference, according to Fig.5b. However, Fig.5a shows that sample A gives a 37% higher MRR than sample B in A-plane sapphire polishing. Three features have been found in particles

of sample A: non-spherical shape, wide size distribution, and incorporated with cobalt. So, very probably, it is the unique shape and wide size distribution that influence the polishing performance.

First, the average COF of different abrasive particles during the CMP process are shown in Fig.5, which is measured by CP-4 system. It's evident that particles with non-spherical shape show a higher COF value. There are two kinds of motion of abrasives particles during chemical mechanical polishing process: sliding and rolling. Non-spherical particles and higher COF means a higher ratio of sliding rather than rolling, inducing a quick remove of the material on the wafers surface<sup>[10,22]</sup>.

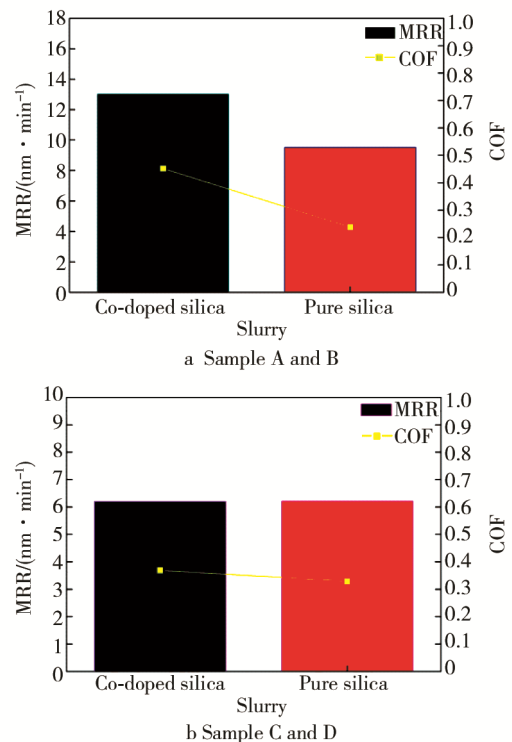


Fig.5 MRR and COF of the different abrasives in A-plane sapphire polishing

图 5 不同磨料在 A 向蓝宝石抛光的抛光速率和摩擦系数数据对比图

Second, numerous interspaces on the pad surface within micro and nano scale are shown in Fig.6. With a wide size distribution, particles will be embedded into the different sized nano-scale asperities on the pad surface during CMP process, forming pad-abrasives to increase the friction between wafers and pad, which in turn increase the material removal rates<sup>[5,23]</sup>.

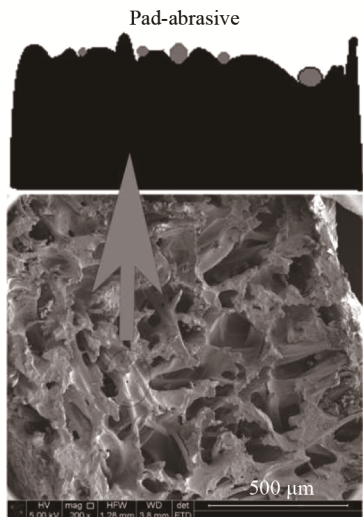


Fig.6 Padsurface and pad-abrasive. 图6 抛光垫表面结构

It's believed that arbitrary shape of particles can cause damages to wafer surface. However, as is shown in Fig.7, things are different in this research. Roughness of wafer surface polished by Co-doped silica and pure silica are similar, which are 0.405 nm and 0.401 nm. The reasons are that, on the one hand, with low hardness and smooth surface, non-spherical silica particles slide without digging or plowing into the surface during CMP process, with few scratches on wafer surface<sup>[24]</sup>. On the other hand, the heat generated by higher friction (Fig.5a) and mechanical action will be helpful to chemical reaction during CMP process. The wafer surface will be perfect when chemical and mechanical actions reach a balanced state.

So it comes to a conclusion that non-spherical Co-doped colloidal silica prepared by cobalt induced method has a 37% higher MRR and a similar smooth surface compared with pure colloidal silica, which means a better CMP performance in A-plane sapphire polishing.

### 2.3 CMP mechanism

Co-doped silica abrasives prepared were used in A-plane sapphire polishing. In order to analyze the CMP mechanism, we investigated the XPS spectra of Co, Al, Si and O of pure silica abrasives and Co-doped

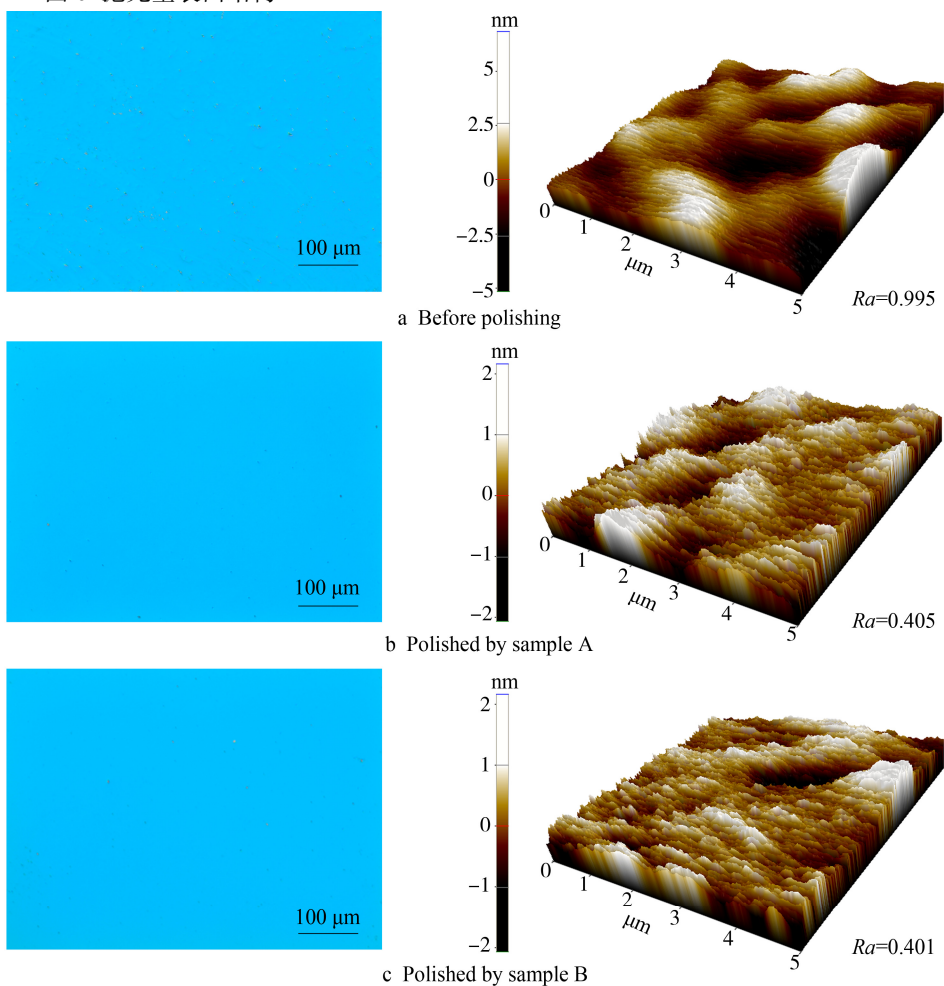


Fig.7 Metalloscope and AFM of the surface 图7 蓝宝石表面的金相显微镜图和AFM图: a)抛光前, b)样品A抛光后, c)样品B抛光后

colloidal silica abrasives before and after polishing were investigated. The abrasives were centrifuged and the residual solid was dried at 50 °C for 72 h for XPS measurement. The result is shown in Fig.8 and the corresponding bind energies are listed in Tab.4.

XPS spectra of Al2p appeared after polishing. The peak at the binding energy of 69.07 eV and 71.75 eV (Fig.8b, Al) corresponds to Al<sub>2</sub>O<sub>3</sub> which come from the sapphire, and the peak at 74.71 eV and 79.81 eV (Fig.8b, Al) belongs to Al<sub>2</sub>Si<sub>2</sub>O<sub>7</sub> and AlOOH, respectively.

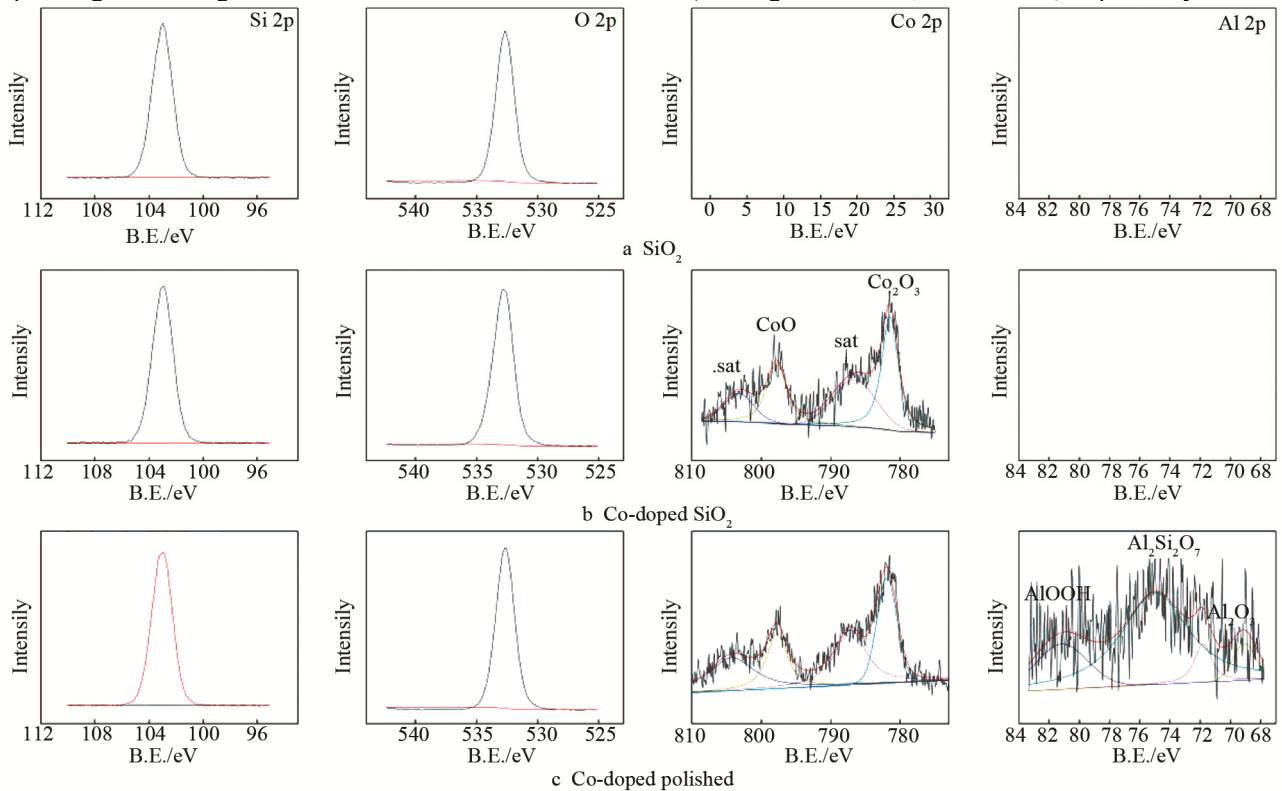


Fig.8 XPS spectra

图 8 XPS 光谱: a) 纯硅溶胶, b) 抛光前的诱导法钴掺杂硅溶胶, c) 抛光后的诱导法钴掺杂硅溶胶

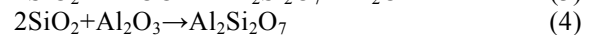
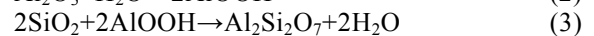
Peak locations of Co haven't shifted after polishing, as are shown in Fig.8.b and Fig.8c. There are two peaks of Co2p, one at the binding energy of 782.11 eV Co2p<sub>3/2</sub> (octahedral), with a satellite peak around 787.01 eV; and the other at the binding energy of 798.07 eV Co2p<sub>1/2</sub> (octahedral), with a side peak around 804.05 eV. The appearance of satellite peaks indicate the absence of CoO, Co<sub>2</sub>O<sub>3</sub> and Co<sub>3</sub>O<sub>4</sub> pure component, and the higher binding energy of Co2p<sub>1/2</sub> and Co2p<sub>3/2</sub> than that of pure component show that Co element exist in the particles in the form of Co—O—Si bond, with Co in an octahedral structure and Si in a tetrahedral structure<sup>[25-27]</sup>.

It seems that peak locations of Si and O haven't changed. However, in the enlarged pictures shown in

Fig.9, we can see the differences. In terms of the Si peaks, first, the Co-doped silica shows a different incline from that of pure SiO<sub>2</sub> at the top of the peak, which is caused by the doping of Co; Second, compared with Co-doped silica, a side peak at 103.25 eV emerge after polishing, indicating the existence of Al<sub>2</sub>Si<sub>2</sub>O<sub>7</sub>, a reaction product between Al<sub>2</sub>O<sub>3</sub> and SiO<sub>2</sub>.

O shows a similar change with Si, mainly belong to SiO<sub>2</sub> and Al<sub>2</sub>Si<sub>2</sub>O<sub>7</sub>.

Upon the XPS analysis, reaction between Co and Al<sub>2</sub>O<sub>3</sub> remains uncertain. Thus the relative reaction can be described as the equations (2—4)<sup>[28]</sup>.



Tab.4 Binding energy of Al, Co, Si and O in abrasive (before and after polishing)

表 4 磨料中 Co, Al, Si 和 O 抛光前后结合能对比

| Element           | Al       |          | Co       |          | Si               |          |          | O                |          |          |
|-------------------|----------|----------|----------|----------|------------------|----------|----------|------------------|----------|----------|
|                   | Polished | Co doped | Polished | Polished | SiO <sub>2</sub> | Co doped | Polished | SiO <sub>2</sub> | Co doped | Polished |
| Binding energy/eV | 69.07    | 782.08   | 782.11   |          |                  |          |          |                  |          |          |
|                   | 71.75    | 786.61   | 787.01   |          |                  |          |          |                  |          |          |
|                   | 74.71    | 797.99   | 798.07   |          | 102.98           | 103.01   | 103.04   | 532.66           | 532.76   | 532.67   |
|                   | 79.81    |          | 805.01   |          |                  |          |          |                  |          |          |

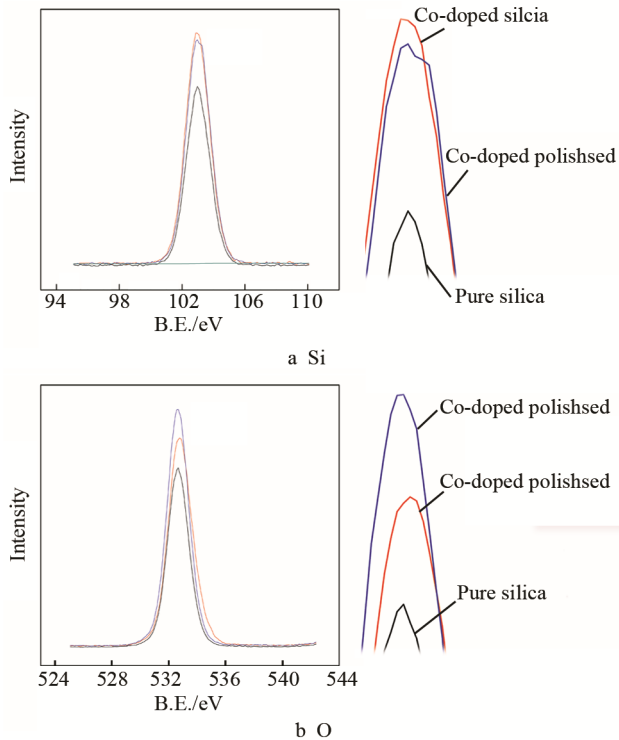


Fig.9 Enlarged picture of XPS peaks before and after polishing

图9 抛光前后 XPS 光谱放大图

### 3 Conclusions

Co-doped colloidal silica with non-spherical and spherical shape were synthesized by cobalt induced method and seeds induced method, respectively. The methods we used in this article are simple and cost saving than what the previous literatures reported. Particles tend to be uniform while grow on spherical seeds in alkaline solution. However, when prepared by cobalt induced method, there are three steps, nucleation, coagulation and further growth of fused particles, which caused the formation of non-spherical silica particles. And according to the XPS spectra and TEM-EDS, Co has been successfully doped in particles in the form of Co—O—Si bond.

We investigated the effects of shape and cobalt element in A-plane sapphire polishing by comparing the MRR of Co-doped and pure colloidal silica prepared by different methods. Non-spherical Co-doped silica particles give a 37% higher MRR in A-plane sapphire polishing because of their non-spherical shape and wide size distribution; while as can be seen from the the CMP performance of spherical Co-doped silica, Co doesn't improve MRR in A-plane sapphire polishing according to the comparison between spherical Co-doped silica and pure silica. In addition, non-spherical particles reach a similar surface *Ra* with pure colloidal silica because of the particles' action mode "slide without digging into the surface" and the balance between chemical reaction and mechanical action. So it's confirmed that the non-spherical Co-doped particles pre-

pared by cobalt induced method give a perfect CMP performance.

### Reference:

- [1] YAN W X, ZHANG Z F, GUO X H, et al. The Effect of pH on Sapphire Chemical Mechanical Polishing[J]. ECS Journal of Solid State Science and Technology, 2015, 4(3): 108-111.
- [2] AIDA H, KIM S W, SUNAKAWA K, et al. III-Nitride Epitaxy on Atomically Controlled Surface of Sapphire Substrate with Slight Misorientation[J]. Japanese Journal of Applied Physics, 2012, 51(2): 5502.
- [3] 彭进, 夏琳, 邹文俊. 化学机械抛光液的发展现状与研究方向[J]. 表面技术, 2012, 41(4): 95-98.
- [4] PENG J, XIA L, ZOU W J. Research Status and Prospect of Chemical Mechanical Polishing Slurry[J]. Surface Technology, 2012, 41(4): 95-98.
- [5] ZHOU Y, PAN G S, GONG H, et al. Characterization of Sapphire Chemical Mechanical Polishing Performances Using Silica with Different Sizes and Their Removal Mechanisms[J]. Colloids and Surface A, 2017, 513: 153-159.
- [6] KONG H, HUO J C, LIANG C L, et al. Polydisperse Spherical Colloidal Silica Particles: Preparation and Application[J]. China Physics B, 2016, 25(11): 613-618.
- [7] LI W W, DIAO J X. The Preparation of Nanometer Non Spherical Colloidal Silica and Its Polishing Character[J]. ECS Transactions, 2013, 52(1): 507-512.
- [8] LIANG C L, WANG L Y, LIU W L, et al. Non-spherical Colloidal Silica Particles—Preparation, Application and Model[J]. Colloids and Surfaces A: Physicochemical and Engineering Aspects, 2014, 457: 67-72.
- [9] LIANG C L, LIU W L, ZHENG Y H, et al. Fractal Nature of Non-Spherical Silica Particles Via Facile Synthesis for the Abrasive Particles in Chemical Mechanical Polishing[J]. Colloids and Surfaces A: Physicochemical and Engineering Aspects, 2016, 500: 146-153.
- [10] MORIOKA Y, KINOSHITA M, HABA S. An Approach to Slurry Characterization for CMP[C]//PacRim-CMP 2004. Tokyo: The Japan Society of Mechanical Engineers, 2004: 153-155.
- [11] WRSCHKA P, HERNANDEZ J, OEHRLEIN G S, et al. Development of a Slurry Employing a Unique Silica Abrasive for the CMP of Cu Damascene Structures[J]. Journal of the Electrochemical Society, 2001, 148(6): 321-325.
- [12] SIVANANDINI M, DHAMI S S, PABLA B S, et al. Effect of 3-mercaptopropyltrimethoxy-silane on Surface Finish and Material Removal Rate in Chemical Mechanical Polishing[J]. Procedia Materials Science, 2014, 6: 528-537.
- [13] LEE C, PARK S H, CHUNG W, et al. Preparation and Characterization of Surface Modified Silica Nanoparticles with Organo-Silane Compounds[J]. Colloids and Surfaces

- A: Physicochemical and Engineering Aspects, 2011, 384(1-3): 318-322.
- [13] LEI H, TONG K Y, WANG Z Y. Preparation of Ce-doped Colloidal SiO<sub>2</sub> Composite Abrasives and Their Chemical Mechanical Polishing Behavior on Sapphire Substrates[J]. Materials Chemistry and Physics, 2016, 172: 26-31.
- [14] LEI H, TONG K Y. Preparation of La-doped Colloidal SiO<sub>2</sub> Composite Abrasives and Their Chemical Mechanical Polishing Behavior on Sapphire Substrates[J]. Precision Engineering, 2016, 44: 124-130.
- [15] LEI H, GU Q, CHEN R L, et al. Preparation of Fe-doped Colloidal SiO<sub>2</sub> Abrasives and Their Chemical Mechanical Polishing Behavior on Sapphire Substrates[J]. Applied Optics, 2015, 54(24): 7188-7194.
- [16] KIM D W, DAI J. Chemical Mechanical Polishing Slurry Composition Including Iron-doped Colloidal Silica: MY, 142487A[P]. 2010-11-30.
- [17] MA P, LEI H, CHEN R L. Preparation of Cobalt-doped Colloidal Silica Abrasives and their Chemical Mechanical Polishing Performances on Sapphire[J]. Micro & Nano Letters, 2015, 10(11): 657-661.
- [18] ZHANG Z F, YAN W X, ZHANG L, et al. Effect of Mechanical Process Parameters on Friction Behavior and Material Removal during Sapphire Chemical Mechanical Polishing[J]. Microelectronic Engineering, 2011, 88(9): 3020-3023.
- [19] BERNE B J, ROBERT P. Laser Light Scattering from Liquids[J]. Annual Review of Physical Chemistry, 1974, 25: 233-253.
- [20] YUASA H, KANESHIGE J, OZEKI T, et al. Application of Acid-Treated Yeast Cell Wall (AYC) as a Pharmaceutical Additive. III. AYC Aqueous Coating onto Granules and Film Formation Mechanism of AYC[J]. International Journal of Pharmaceutics, 2002, 237(1-2): 15-22.
- [21] SUN Z Y, XU S H, DAI G L, et al. A Microscopic Approach to Studying Colloidal Stability[J]. Journal of Chemical Physics, 2003, 119(4): 2399-2405.
- [22] LEE H, KIM M, JEONG H. Effect of Non-spherical Colloidal Silica Particles on Removal Rate in Oxide CMP[J]. International Journal of Precision Engineering and Manufacturing, 2015, 16(13): 2611-2616.
- [23] SHIH Z W, CHANG K Y, TSENG C L, et al. Method for Preparing Shape-changed Nanosize Colloidal Silica: US, 20030113251A1[P]. 2003-06-19.
- [24] NEGRYCH J A, HAAG G, RALL P E, et al. Abrasive Media and Aqueous Slurries for Chemical Mechanical Polishing and Planarization: US, 6334880B1[P]. 2002-01-01.
- [25] 姜鹤. 钴掺杂氧化物材料的微观结构与磁学行为[D]. 北京: 清华大学, 2012.
- JIANG H. Microstructure and Magnetic Behavior of Oxides Doping with Cobalt[D]. Beijing: Tsinghua University, 2012.
- [26] ERNST B, BENSADDIK A, HILAIRE L, et al. Study on a Cobalt Silica Catalyst during Reduction and Fischer-tropsch Reaction: In situ EXAFS Compared to XPS and XRD[J]. Catalysis Today, 1998, 39(4): 329-341.
- [27] ZHANG Z G, WANG X X, LIU B X, et al. Influence of Preparation Condition on Particles Size and Pore Structure of Cobalt-doped Silica Membrane Sol[J]. Journal of the Chinese Ceramic Society, 2015, 43(4): 458-464.
- [28] ZHOU Y, PAN G S, SHI X L, et al. AFM and XPS Studies on Material Removal Mechanism of Sapphire Wafer during Chemical Mechanical Polishing (CMP)[J]. Journal of Material Science: Material in Electronics, 2015, 26(12): 9921-9928.